A New Boundary Description in Two-Dimensional TLM Models of Microwave Circuits

Zhizhang Chen, Michel M. Ney, *Member, IEEE*, and Wolfgang J. R. Hoefer, *Senior Member, IEEE*

Abstract—**In this paper, we describe a new boundary representation for the two-dimensional transmission line matrix method of numerical analysis (TLM). In conventional TLM simulations, boundary conditions are realized by introducing the appropriate impulse reflection coefficients halfway between two nodes. Since the total field quantities are defined on the nodes, their values at the boundary are not directly available from TLM solutions. We have thus modified the TLM procedure so that boundaries can be placed across the nodes. The boundary conditions in TLM can then be formulated in terms of the field boundary conditions derived from Maxwell's equations, rather than in terms of impulse reflection coefficients. The essential differences between the conventional TLM and our proposed procedure are presented. Examples are given for several typical problems, and the results obtained with the two methods are compared. These were found to be in excellent agreement.**

I. Introduction

THE theory of the two-dimensional TLM and its application to electromagnetic problems have been well established [1]–[5] since its formulation by Johns and his coworkers. Electromagnetic fields are modeled by filling the field space with a network of transmission lines; this renders the problem discrete in space and time since impulses launched on the network are scattered at all nodes at a fixed time step sequence. The voltages and currents at all nodes are equivalent to the electric and magnetic fields in the discretized space. Thus the behavior of electromagnetic fields can be easily modeled quantitatively by the voltages and currents in the appropriate TLM models. This makes the TLM method a very powerful numerical technique for solving electromagnetic problems with computers.

In the two-dimensional TLM network shown in Fig. 1, traditional boundary conditions are realized by placing the boundaries halfway between two nodes and modeling them by appropriate reflection and transmission coefficients. A wide range of problems have been solved successfully with this boundary description [1]–[3]. However, since the closest nodes are $\Delta l/2$ away from the boundaries and since fields are defined at the nodes, the field quantities on the boundaries cannot be obtained directly from the TLM solutions.

This paper introduces a technique by which the boundaries are placed across the nodes rather than halfway between them. Therefore, the boundary conditions can be formulated in terms of the total fields governed by Maxwell's equations, rather than in terms of impulse reflection and transmission coefficients. This makes the boundary description in TLM compatible with that of other numerical methods and analytical approaches, even though the modeling of wave propagation is governed by Huygens's principle. The new boundary description proposed in this paper thus facilitates the combination of TLM with other methods such as analytical and finite difference approaches for absorbing boundary modeling. Finally, one can also use it in combination with the conventional TLM boundary scheme, thus doubling the resolution of TLM boundary treatment.

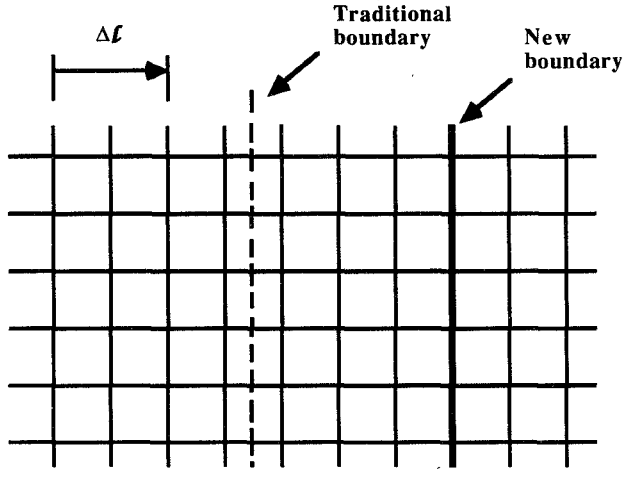

Fig. 1. The placement of a traditional and of the newly proposed boundary in TLM network.

II. The New TLM Boundary Description

From Maxwell's equations, the following general field boundary conditions are derived:

1) On a perfect reflecting wall C (Fig. 2), the electric and magnetic fields must satisfy the following conditions:

$$\boldsymbol{n} \times \boldsymbol{E} = 0 \tag{1}$$

$$\boldsymbol{n} \cdot \boldsymbol{H} = 0 \tag{2}$$

if C is an electric wall, and

$$\boldsymbol{n} \times \boldsymbol{H} = 0 \tag{3}$$

$$\boldsymbol{n} \cdot \boldsymbol{E} = 0 \tag{4}$$

if C is a magnetic wall.

Manuscript received May 3, 1990; revised October 3, 1990.

The authors are with the Department of Electrical Engineering, University of Ottawa, Ottawa, Canada K1N 6N5.

IEEE Log Number 9041961.

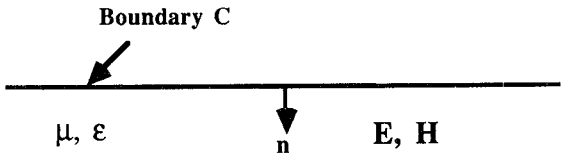

Fig. 2. A perfect reflecting boundary C.

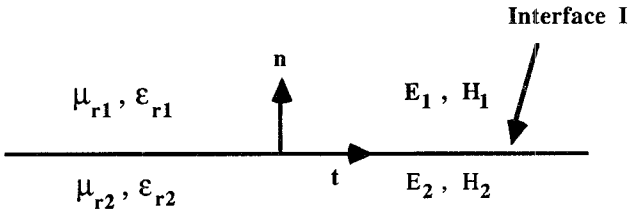

Fig. 3. An interface between two dielectric regions.

2) On the interface I between the two dielectric regions (Fig. 3), the electric and magnetic fields must satisfy the following conditions:

$$E_{t1} = E_{t2} \tag{5}$$

$$H_{t1} = H_{t2}. \tag{6}$$

In a TLM model, the voltages and currents at the nodes are equivalent to the electric and magnetic fields in the real structure. Therefore, by imposing the above field boundary conditions upon the voltages and currents on the boundary or interface nodes of the TLM model, the new boundary representation can be easily obtained. In the following section, this procedure will be discussed for the case of two-dimensional TLM shunt-connected networks.

A. Representation of Perfect Electric Walls

Consider the empty half-space bounded by a perfect electric wall to the $y-z$ plane, as shown in Fig. 4(a). Assuming that $\partial/\partial y = 0$, we can model this half-space by a shunt-connected 2-D TLM mesh in which the node voltage, V_y, simulates the y component of the electric field, E_y, (Fig. 4(b)). In contrast to the conventional arrangement, the mesh position is such that a row of nodes coincides with the electric wall.

The boundary condition, $E_y = 0$, is now simulated by numerically forcing V_y to vanish at each iteration at all boundary nodes. Referring to Fig. 4(c), the value of V_y at the kth iteration is [5]

$${}_kV_y = \frac{1}{2}\left({}_kV_1^i + {}_kV_2^i + {}_kV_3^i + {}_kV_4^i\right) = 0$$

(at the boundary nodes) (7)

where ${}_kV_j^i$ is the incident voltage on the jth branch of the node on the boundary at the kth iteration.

Since in this case, ${}_kV_1^i$, ${}_kV_2^i$, and ${}_kV_4^i$ have been computed at the previous iteration, the impulse ${}_kV_3^i$ to be injected via the "outside branch" is

$${}_kV_3^i = -\left({}_kV_1^i + {}_kV_2^i + {}_kV_4^i\right). \tag{8}$$

Once ${}_kV_3^i$ is determined, the "reflected" impulse voltages on the four branches are obtained in the same way as at all the other nodes of the mesh. The impulse ${}_{k+1}V_3^r$ leaving the boundary node via the outside branch is simply absorbed by a matched load.

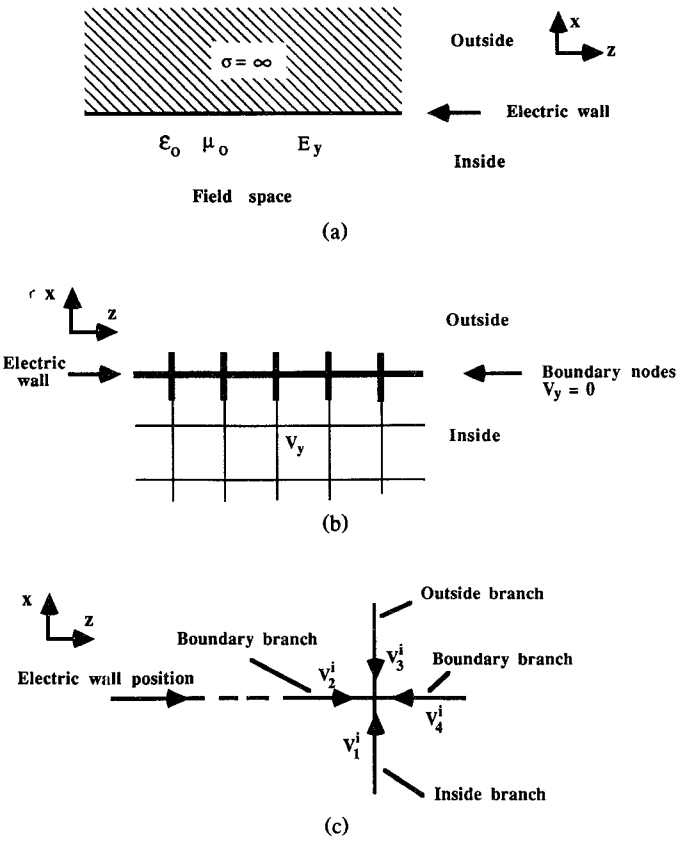

Fig. 4. Modeling of an electric wall by a row of boundary nodes in a shunt-connected 2-D TLM mesh (The node voltage V_y simulates the electric field E_y). (a) Electric wall bounding the field space. (b) Shunted connected 2-D TLM mesh with a row of boundary nodes along the position of the electric wall. (c) The branches of a boundary node.

Note that this boundary description is a purely numerical procedure, performed only at discrete node locations along the boundary. The TLM mesh lines that lie in the boundary plane (boundary branches) are not physically short-circuited by the wall (except at the nodes). On the contrary, they form an integral part of the TLM network and carry the tangential fractions of the discretized Huygens waves emanating from the boundary nodes. It can be shown easily that this boundary algorithm conserves the energy in the system. The reflected impulse voltage ${}_{k+1}V_3^r$ absorbed in the outside branch at each iteration is [5]

$${}_{k+1}V_3^r = \frac{1}{2}\left({}_kV_1^i + {}_kV_2^i + {}_kV_3^i + {}_kV_4^i\right) - {}_kV_3^i. \tag{9}$$

Replacing ${}_kV_3^i$ in the bracket by (8), we obtain

$${}_{k+1}V_3^r = -{}_kV_3^i \tag{10}$$

and since the energy content of each impulse is proportional to the square of the voltage, the energy lost at each iteration at a boundary node is indeed equal to the energy injected, thus ensuring conservation.

The boundary treatment can be generalized for a 2-D TLM mesh which is equipped with permittivity and lossy stubs. A boundary node in such a mesh is shown in Fig. 5.

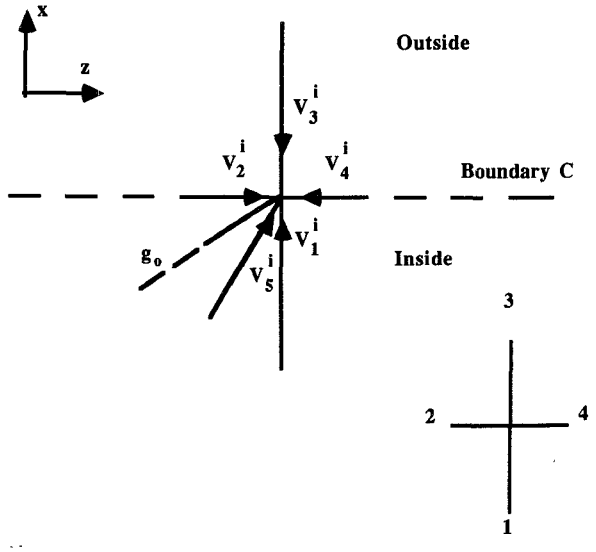

Fig. 5. A boundary node equipped with a permittivity and a lossy stub.

Again, the node voltage ${}_kV_y$ [5] must vanish at each iteration:

$$ {}_kV_y = \frac{2}{y}\left({}_kV_1^i + {}_kV_2^i + {}_kV_3^i + {}_kV_4^i + y_o\,{}_kV_5^i\right) \tag{11} $$

which yields the impulse voltage to be injected via the "outside" branch as

$$ {}_kV_3^i = -\left({}_kV_1^i + {}_kV_2^i + {}_kV_4^i + y_o\,{}_kV_5^i\right) \tag{12} $$

where ${}_kV_j^i$ is the incident voltage on the jth branch of the node on the boundary at the kth iteration ($j=1,\cdots,5$), $y=4+y_o+g_o$, y_o is the normalized characteristic admittance of the permittivity stub, and g_o is the normalized characteristic admittance of loss stub. In both case, the normalizing admittance is the characteristic admittance of the link lines.

Since there exists a dual two-dimensional TLM model in which the currents correspond to the electric fields, we have [5]

$$ {}_kE_z = {}_kI_x = {}_kV_3^t - {}_kV_1^i = 0 \tag{13} $$

which leads to

$$ {}_kV_3^t = {}_kV_1^i. \tag{14} $$

Equations (12) and (14) are the new boundary descriptions for a perfect electric wall in which the unknown incident voltage ${}_kV_3^i$ injected via an outside branch is determined in terms of the incident voltages on the other branches, rather than in terms of reflection coefficients.

B. Representation of Perfect Magnetic Walls

A similar arrangement can be made for perfect magnetic walls, where the normal component of the electric field or the tangential component of the magnetic field must vanish. If the boundary C in Fig. 4 is a perfect magnetic wall, we can set

$$ {}_kV_3^t = {}_kV_1^t \tag{15} $$

where the currents in the TLM mesh correspond to magnetic fields, and

$$ {}_kV_3^i = -\left({}_kV_1^i + {}_kV_2^i + {}_kV_4^i + y_o\,{}_kV_5^t\right) \tag{16} $$

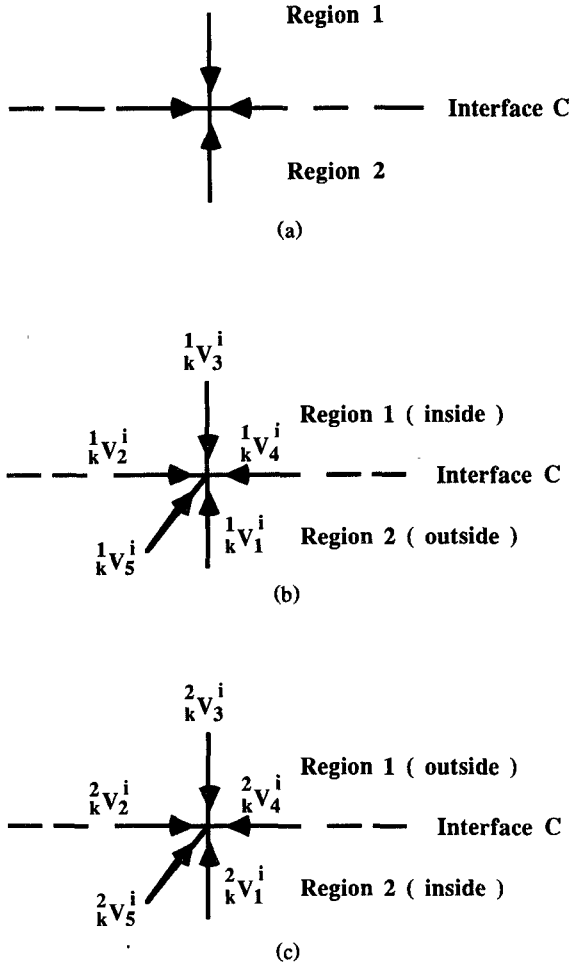

Fig. 6. (a) The inferface of two regions. (b) TLM network for region 1 on the interface. (c) TLM network for region 2 on the interface.

where the voltages in the TLM mesh correspond to the magnetic fields.

It is obvious that (15) and (16) are similar to (12) and (14), given the dual properties of electric and magnetic walls. Thus, only two formulas are needed in the new boundary representation to describe both electric and magnetic walls.

C. Representation of Interfaces Between Dielectric Regions

In the case of two dielectric regions (Fig. 6), two separate TLM networks for modeling region 1 and region 2 are needed. The connection of the two TLM networks on the interface should be consistent with the field boundary conditions, (5) and (6). Also, we must account for the dual TLM models.

When the electric fields are equivalent to the voltages in the TLM mesh [5], we have

$$ {}_kE_{1t} = {}_kV_{1y} = \frac{2}{y_1}\left({}^1_kV_1^i + {}^1_kV_2^t + {}^1_kV_3^t + {}^1_kV_4^t + {}_1y_o\,{}^1_kV_5^i\right) \tag{17} $$

$$ {}_kH_{1t} = {}_kI_{1x} = {}^1_kV_3^t - {}^1_kV_1^i \tag{18} $$

$$ {}_kE_{2t} = {}_kV_{2y} = \frac{2}{y_2}\left({}^2_kV_1^t + {}^2_kV_2^t + {}^2_kV_3^t + {}^2_kV_4^t + {}_2y_o\,{}^2_kV_5^t\right) \tag{19} $$

$$ {}_kH_{2t} = {}_kI_{2x} = {}^2_kV_3^t - {}^2_kV_1^t \tag{20} $$

where ${}^n_k V^i_j$ is the incident voltage on branch j in the TLM network for region n ($n=1,2$, and $j=1,\cdots,5$) at the kth iteration. Also, $y_n = 4 + {}_n y_o + {}_n g_o$, where ${}_n y_o$ is the normalized characteristic admittance of the permittivity stub for region n, and ${}_n g_o$ is the normalized characteristic admittance of the lossy stub of the TLM network for region n.

In order to satisfy the continuity conditions of the tangential component for the electric fields on the interface,

$$ {}_k V_{1y} = {}_k V_{2y} \tag{21} $$

$$ {}_k I_{1x} = {}_k I_{2x} \tag{22} $$

which leads to the following boundary representations:

$$ {}^1_k V^i_1 = (p+q)/(s+1) \tag{23} $$

$$ {}^2_k V^t_3 = (sq-p)/(s+1) \tag{24} $$

where

$$ s = y_2/y_1 $$

$$ p = \left({}^2_k V^i_1 + {}^2_k V^i_2 + {}^2_k V^t_4 + {}_2 y_o \, {}^2_k V^t_5\right) - s\left({}^1_k V^i_2 + {}^2_k V^i_3 + {}^2_k V^i_4 + {}_1 y_o \, {}^1_k V^i_5\right) $$

and

$$ q = {}^1_k V^t_3 + {}^2_k V^t_1. $$

When the magnetic fields are equivalent to the voltage on the TLM mesh [5],

$$ {}_k H_{1t} = {}_k V_{1y} = \frac{2}{y_1}\left({}^1_k V^i_1 + {}^1_k V^t_2 + {}^1_k V^t_3 + {}^1_k V^i_4 + {}_1 y_o \, {}^1_k V^i_5\right) \tag{25} $$

$$ {}_k E_{1t} = {}_k I_{1x}/\epsilon_{r1} = \left({}^1_k V^t_3 - {}^1_k V^i_1\right)/\epsilon_{r1} \tag{26} $$

$$ {}_k H_{1t} = {}_k V_{2y} = \frac{2}{y_2}\left({}^2_k V^i_1 + {}^2_k V^t_2 + {}^2_k V^t_3 + {}^2_k V^t_4 + {}_2 y_o \, {}^2_k V^i_5\right) \tag{27} $$

$$ {}_k E_{1t} = {}_k I_{1x}/\epsilon_{r2} = \left({}^2_k V^t_3 - {}^2_k V^i_1\right)/\epsilon_{r2}. \tag{28} $$

The field boundary conditions of the interface require that

$$ {}_k V_{1y} = {}_k V_{2y} \tag{29} $$

$$ {}_k I_{1x}/\epsilon_{r1} = {}_k I_{2x}/\epsilon_{r2} \tag{30} $$

which leads to the following:

$$ {}^1_k V^t_1 = \frac{p+q}{s_1+s_2} \tag{31} $$

$$ {}^2_k V^i_3 = \frac{s_1 q - s_2 p}{s_1+s_2} \tag{32} $$

where

$$ s_1 = y_2/y_1 \qquad s_2 = \epsilon_{r2}/\epsilon_{r1} $$

$$ p = \left({}^2_k V^t_1 + {}^2_k V^t_2 + {}^2_k V^t_4 + {}_2 y_o \, {}^2_k V^i_5\right) - s_1\left({}^1_k V^i_2 + {}^1_k V^t_3 + {}^1_k V^t_4 + {}_1 y_o \, {}^1_k V^t_5\right) $$

and

$$ q = s_2 \, {}^1_k V^i_3 + {}^1_k V^i_1. $$

Equations (23), (24) and (31), (32) are the new interface conditions formulated for two adjacent dielectric regions. Equations (23) and (24) represent the special case of (31) and (32) when $s_2 = 1$. Therefore, only two formulas are needed to describe the interface conditions between two dielectric regions.

So far, the new TLM boundary representations have been derived for dielectric interfaces and for ideal electric and magnetic walls. By following a similar procedure, it is not difficult to obtain the new boundary formulas for the series node network and for other kinds of boundary conditions, for example the interface conditions between two regions with two different permeabilities. In addition, it is expected that the new boundary conditions can be expanded by lossy boundaries, to three-dimensional TLM analysis, and to TLM models used in other areas such as thermodynamics, optics, and acoustics.

Generally speaking, even though voltage impulses are continuously injected into the boundary nodes, no additional errors or instabilities are created, which means that the energy remains conserved. According to the uniqueness theorem of electromagnetic theory, the fields in a region can be uniquely determined by the sources inside the region and by the fields on the boundary. Since the voltages and currents in TLM simulate the electric and magnetic fields, the TLM solutions can be determined uniquely if the finite sources and boundary representations of the TLM model are known. This ensures that the new boundary representation yields a correct and stable solution.

III. Numerical Results

The new boundary description has been verified by applying it to three typical problems and comparing the results with values obtained from the conventional TLM method [1]–[3] using the same mesh size and number of iterations.

Fig. 7(b) gives the normalized cutoff frequencies for TM modes in a square waveguide with sizes $10\,\Delta l$, shown in Fig. 7(a). The slow-wave properties of the transmission-line matrix automatically give the solutions for a medium of relative permittivity 2 within the guide. This calculations have been performed for 500 iterations.

Fig. 8(b) shows the normalized cutoff frequencies of the dominant mode of the simple inhomogeneously filled waveguide in Fig. 8(a) computed with 100 iterations. The results are compared with the reference values used by Johns [3]. The width of the guide ranges from $5\,\Delta l$ to $20\,\Delta l$, with a dielectric permittivity of 2.45. The interface conditions described in subsection II-C have been applied.

Fig. 9(b) shows the normalized dominant cutoff frequency of the finned waveguide in Fig. 9(a) obtained with three different methods. The analytical results were obtained with the transverse resonance methods. In this method, the TLM with the new boundary representation gives a more accurate solution than the conventional TLM. This may be explained by the fact that one node placed on the conductor edge produces large (but not infinite) field values. This certainly contributes to a better field description around the fin, thereby yielding a better accuracy for parameter evaluations.

The above results show that the TLM with the new boundary representation gives results similar in accuracy to those obtained with the traditional boundary representation. Furthermore, it has been verified by calculations that the solutions with the new boundary representation converge to the exact solutions when the number of iteration is increased, indicating that the new boundary description does not introduce convergence problems, instability, or spurious solutions

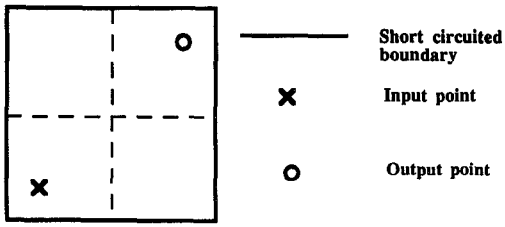

(a)

NORMALIZED CUTOFF FREQUENCY OF HIGH ORDER MODES IN SQUARE WAVEGUIDE

Mode	Result from this method	Result from conventional TLM	Analytical result	Error of this method	Error of conventional TLM
	$\Delta\ell/\lambda$	$\Delta\ell/\lambda$	$\Delta\ell/\lambda$	%	%
TM_{12}	0.0788	0.0788	0.0791	0.38	0.38
TM_{22}	0.0999	0.0999	0.1000	0.10	0.10
TM_{13}	0.1105	0.1104	0.1118	1.34	1.25
TM_{23}	0.1270	0.1269	0.1275	0.39	0.47
TM_{14}	0.1418	0.1414	0.1458	2.74	3.02
TM_{33}	0.1499	0.1498	0.1550	0.07	0.13
TM_{24}	0.1558	0.1558	0.1581	1.45	1.45
TM_{34}	0.1760	0.1760	0.1768	0.45	0.45
TM_{25}	0.1840	0.1841	0.1904	3.36	3.31
TM_{44}	0.1997	0.1996	0.2000	0.15	0.20

Maximum truncation error not greater than 0.2 %

Dimensions 10 $\Delta\ell$

(b)

Fig. 7. (a) Geometry for higher order modes in a square-cross-section waveguide. (b) Normalized cutoff frequencies of high-order modes in the square waveguide.

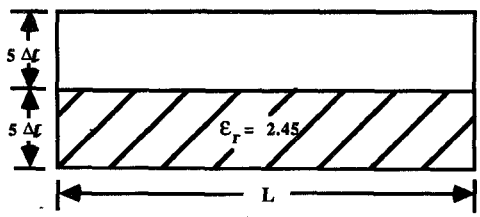

(a)

NORMALIZED CUTOFF FREQUENCIES OF QUASI - H_{10} MODE IN INHOMOGENEOUSLY FILLED RECTANGULAR CAVITY

Guide width L	Result from this method	Result from conventional [3]	Analytical result [3]	Maximum truncation error	Maximum velocity error
$\Delta\ell$	$\Delta\ell/\lambda$	$\Delta\ell/\lambda$	$\Delta\ell/\lambda$	%	%
5	0.0784	0.0781	0.0791	0.4	0.4
6	0.0690	0.0692	0.0693	0.6	1.6
7	0.0621	0.0625	0.0630	0.8	1.2
10	0.0518	0.0518	0.0518	1.2	0.9
20	0.0411	0.0413	0.0415	1.8	0.5

ε_r = 2.45

(b)

Fig. 8. (a) Two-dimensional inhomogeneously filled rectangular cavity. (b) Normalized cutoff frequencies of quasi-H_{10} mode in the rectangular cavity.

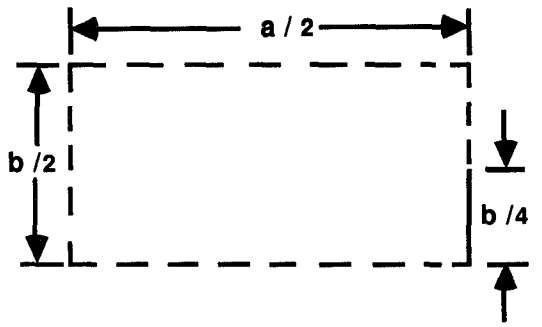

(a)

NORMALIZED CUTOFF FREQUENCY OF THE FINNED WAVEGUIDE

Result of this method	Result of conventional	Analytical result
b/λ	b/λ	b/λ
0.224	0.206	0.225

$a/b = 2$, $b/\Delta l = 12$

(b)

Fig. 9. (a) Geometry of the finned waveguide. (b) Normalized cutoff frequency of the finned waveguide.

and thus is not inferior to the traditional boundary formulation.

IV. Conclusion

In this paper, we have presented a new TLM boundary description where the boundaries are placed across the nodes of the TLM network. Thus the boundary conditions are specified in terms of field boundary conditions, rather than in terms of reflection and transmission coefficients, which means that the field value at the boundary can be directly incorporated into the TLM model. This considerably increases the flexibility and versatility of TLM simulations since the new boundary description is more compatible with methods based on partial differential equations. For example, the TLM with the new boundary representation may be easily adopted to solve unbounded wave problems, or it can be combined more easily with analytical methods or the time-domain finite-difference method, etc. Thus it facilitates interfacing TLM with other approaches when dealing with open field problems or with situations which are handled more effectively with alternative methods.

References

[1] P. B. Johns and R. L. Beurle, "Numerical solution of 2-dimensional scattering problems using a transmission-line matrix," *Proc. Inst. Elec. Eng.*, vol. 118, no. 9, pp. 1203–1208, Sept. 1971.

[2] P. B. Johns, "Application of the transmission-line matrix method to homogeneous waveguides of arbitrary cross-section," *Proc. Inst. Elec. Eng.*, vol. 119, no. 8, pp. 1086–1091, Aug. 1972.

[3] P. B. Johns, "The solution of inhomogeneous waveguide problems using transmission-line matrix," *IEEE Trans. Microwave Theory Tech.*, vol. MTT-22, pp. 209–215, Mar. 1974.
[4] W. J. R. Hoefer, "The transmission-line matrix method-theory and application," *IEEE Trans. Microwave Theory Tech.*, vol. MTT-33, pp. 882–893, Oct. 1985.
[5] W. J. R. Hoefer, "The transmission line matrix (TLM) method," in *Numerical Techniques for Passive Microwave and Millimeter-Wave Structures*, T. Itoh, Ed. New York: Wiley, 1989, ch. 8, pp. 486–591.

Zhizhang Chen was born in Fujian, People's Republic of China, on July 3, 1962. He received the B.Eng. degree in electrical engineering from Fuzhou University, Fujian, in 1982 and the M.Eng. degree in electrical engineering from the Nanjing Institute of Technology, Nanjing, China, in 1985.

From 1985 to 1988, he was with Fuzhou University, where he did research on satellite–earth direct receivers and taught courses in the area of microwaves. Currently, he is working toward the Ph.D. degree at the University of Ottawa, Ottawa, Canada. His research interests include the propagation and scattering of electromagnetic waves and the design of microwave devices using numerical and analytical methods.

Michel M. Ney (S'80–M'83) received the Engineer Diploma from the Swiss Federal Institute of Technology, Lausanne, Switzerland, in 1976 and the Ph.D. degree from the University of Ottawa in 1983.

Since that time he has been with the Laboratory for Electromagnetics and Microwaves of the Department of Electrical Engineering at the University of Ottawa, where he is presently an Associate Professor. His research interests include passive millimeter-wave circuit design, electromagnetic engineering, electromagnetic interference and compatibility problems (EMI/C), and numerical modeling.

Dr. Ney is a registered professional engineer in the province of Ontario, Canada.

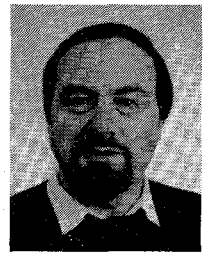

Wolfgang J. R. Hoefer (M'71–SM'78) received the diploma in electrical engineering from the Technische Hochschule Aachen, Germany, in 1965 and the D.Ing. degree from the University of Grenoble, France, in 1968.

After one year of teaching and research at the Institut Universitaire de Technologie, Grenoble, France, he joined the Department of Electrical Engineering at the University of Ottawa, Canada, where he is currently a professor. His sabbatical activities have included six months with the Space Division of AEG-Telefunken in Backnang, Germany, six months with the Electromagnetics Laboratory of the Institut National Polytechnique de Grenoble, France, and one year with the Space Electronics Directorate of the Communications Research Center in Ottawa, Canada. His research interests include microwave measurement techniques, computer-aided design of microwave and millimeter-wave circuits, and numerical techniques for modeling electromagnetic fields.

Dr. Hoefer is a registered professional engineer in the province of Ontario, Canada.